Structure and Dynamics of Concentrated Solutions of Asymmetric Block Copolymers in Slightly Selective Solvents

T. P. Lodge,* X. Xu,† and C. Y. Ryu

Department of Chemistry and Department of Chemical Engineering & Materials Science, University of Minnesota, Minneapolis, Minnesota 55455-0431

I. W. Hamley*

School of Chemistry and Centre for Self-Organising Molecular Systems, University of Leeds, Leeds, W. Yorkshire LS2 9JT, U.K.

J. P. A. Fairclough and A. J. Ryan‡

Manchester Materials Science Centre, UMIST, Grosvenor Street, Manchester M1 7HS, U.K.

J. S. Pedersen

Department of Solid State Physics, Risø National Laboratory, Roskilde DK-4000, Denmark

Received March 21, 1996; Revised Manuscript Received June 12, 1996[⊗]

ABSTRACT: The structural and dynamic properties of a styrene−isoprene−styrene (SIS) triblock copolymer, with block molecular weights of 10^4, 10^5, and 10^4, respectively, and the matching styrene−isoprene (SI) diblock, with block molecular weights of 10^4 and 5×10^4, respectively, are examined in the selective solvent di-*n*-butyl phthalate (DBP). DBP is a good solvent for PS, but a very poor solvent for PI; PI/DBP solutions exhibit a critical temperature near 80 °C. In dilute solution, the triblock copolymer forms micelles with a hydrodynamic radius of 260 Å, which melt at 49 °C. In this work, solutions were polymer concentrations near 20% are emphasized. Small-angle X-ray scattering (SAXS) indicates that below 0 °C, the copolymers form elongated micelles, with isoprene-rich cores. Detailed analysis with an ellipsoidal micelle model suggests core minor radii on the order of 150−200 Å and overall average lengths greater than 1000 Å. As the solutions are heated from *ca.* 10 °C to *ca.* 40 °C, the dynamic shear moduli, G' and G'', increase by as much as 2 orders of magnitude. This is attributed to the swelling of the micelles, as the solvent begins to penetrate the micelle cores, leading to substantial steric interactions between micelles. Upon further heating, the moduli drop sharply, until by about 60 °C they correspond to values for disordered, entangled solutions. The temperature at which the moduli first decrease signals a microphase separation transition (MST), as the micelles disintegrate. The locations of the SAXS structure factor peaks are also consistent with micelle overlap just prior to the MST. Oscillatory flow birefringence measurements indicate the same MST, but below the transition the birefringence is very large, and independent of frequency. This originates from form birefringence, due to the alignment of highly anisotropic micelles. Small-angle neutron scattering under shear also indicates alignment of anisotropic aggregates. In the region between the MST and *ca.* 60 °C, the strong temperature dependences of the moduli, flow birefringence, and scattering intensities are consistent with loose associations among the chains, reminiscent of the fluctuation regime in diblock copolymer melts.

Introduction

The structural and dynamic properties of block copolymer liquids are of great current interest.[1−3] Previous work has tended to emphasize either the melt, where the details of the ordered phase microstructure continue to fascinate, or dilute solutions, where solvent selectivity drives micellization. In contrast, the behavior in concentrated solutions has been less extensively studied.[4−7] Two general issues that remain largely unexplored are the effect of addition of a neutral solvent on the melt phase diagram, *i.e.*, in concentrated solutions, and the additional role played by solvent selectivity. In this paper we address the latter, with the particular examples of triblock and diblock copolymers (of the same, asymmetric composition) in concentrated solutions ($c \approx 0.2$ g/mL), where the solvent is worse than, but close to, a Θ solvent for the middle block. Consequently, small increases in temperature can produce large changes in solution properties. The opposite case, where the solvent prefers the middle block, has also been of interest, because both compact micelles and network structures may be achieved.[8,9]

ABA copolymers in solvents selective for the end blocks have been examined previously by several groups.[1] (In the literature, "selective for" one block usually indicates a nonsolvent for the other block. We use "selective solvent" to denote a solvent that has any differential affinity for the two blocks, but include the modifier "slightly" for systems in which the solvent may dissolve both blocks.) The structure of the resulting micelles has been examined in detail in dilute solution,[10−17] and in particular Tuzar and Kratochvil used mixed solvents to vary the solvent selectivity in a systematic way.[10] Theoretical treatments of the key features (*e.g.*, micelle radius, shape, aggregation number, and cmc) have also been presented.[13,18] In general, one finds that triblocks form spherical micelles under conditions similar to those for the corresponding diblocks, but with smaller aggregation numbers.

Studies of similar systems but at nondilute concentrations have been few. Plestil *et al.* showed that styrene-hydrogenated butadiene−styrene triblocks in

* To whom correspondence should be addressed.
† Current address: Lectec Corp., Minnetonka, MN 55343.
‡ Also: CLRC Daresbury Laboratory, Warrington WA4 4AD, U.K.
⊗ Abstract published in *Advance ACS Abstracts,* August 1, 1996.

S0024-9297(96)00440-8 CCC: $12.00

dioxane/hexane mixtures exhibited a strong increase in viscosity with increasing c, for $c \approx 0.1$ g/mL.[14] This was clearly attributable to micelle−micelle interactions, but there was no evidence of a macrolattice. It was also noted that in this mixed-solvent system hexane could preferentially swell the micelle core. In a series of pioneering papers, Watanabe and Kotaka examined the structure and viscoelastic properties of styrene−diene diblock copolymers over a wide range of concentration and molecular weight.[19] Of particular interest is their observation of a regular periodic structure ("macrolattice") adopted by the micelles at sufficiently high concentrations, and a corresponding regime of plastic behavior in the rheology.

Most recently, considerable attention has been directed to ethylene oxide−propylene oxide−ethylene oxide (Pluronic) copolymers in aqueous solution.[20−23] Here, the solubility of the polymer decreases with increasing temperature, and the selectivity of the solvent toward the end blocks encourages micellization. Phase diagrams have been constructed via experiment[20,21] and theory,[22] which extend up to substantial concentrations. For a semidilute solution, the general sequence dispersed chains → spherical micelles → rodlike micelles → phase separation is anticipated, as temperature is increased. Experimentally, the spherical micellar phase was observed to adopt a bcc macrolattice at an elevated concentration ($c > 0.2$ g/mL).[20,21] The sphere−rod transition is also interesting and has been confirmed to occur upon heating even in dilute solution.[20,23] This aqueous system has an LCST character, and thus, qualitatively, the temperature dependence should be inverse to that observed for organic copolymers such as the styrene−dienes. Indeed, melts and concentrated solutions of diblock copolymers in the hexagonal cylinder phase at a given temperature have been observed to transform to spheres on a bcc lattice upon heating, and in some cases the order−disorder transition (ODT) has been attained for the same specimen.[24−26] This transition reflects the fact that as the A−B interactions become less favorable upon cooling, a sharper A−B interface is preferred. The concomitant stretching of the core chains drives the change in morphology.

In this paper we examine concentrated solutions of a poly(styrene-*b*-isoprene-*b*-styrene) (SIS) triblock and matched diblock copolymer, in the slightly selective solvent di-*n*-butyl phthalate (DBP). Temperature is the primary variable. At or below room temperature, both X-ray scattering (SAXS) and the viscoelastic properties are consistent with a solution of micelles. Furthermore, the micelles are shown to be elongated, *i.e.*, prolate ellipsoids. However, over the approximate range 10−45 °C, the shear moduli increase by up to 2 orders of magnitude, indicating the onset of strong intermicellar interactions. This is attributable to increases in micellar size due to solvent swelling of the core. At a particular temperature near 45 °C, the moduli begin to decrease abruptly, in a manner resembling the signature of the ODT in block copolymer melts. However, it is not until still higher temperatures (*ca.* 60 °C) that the fluid behaves as a truly disordered (albeit entangled) polymer solution. Cloud point studies on DBP solutions of an isoprene homopolymer indicate a critical temperature near 80 °C, lending further support to the hypothesis that changing solvent quality is the primary cause of these phenomena. In addition to rheology and SAXS, small-angle neutron scattering (SANS), oscillatory flow birefringence (OFB), and dynamic light scattering (DLS) are used to investigate the details of these various transformations.

Experimental Section

Samples and Solutions. A poly(styrene-*b*-isoprene-*b*-styrene) triblock, and the matching poly(styrene-*b*-isoprene) diblock, were provided by D. Handlin (Shell Development Co.). The nominal block molecular weights were 1×10^4, 1×10^5, and 1×10^4 for the triblock and 1×10^4 and 5×10^4 for the diblock, with polydispersities of less than 1.06. The samples were thus designated SIS-120 and SI-60 and used without further treatment. The solvent, di-*n*-butyl phthalate (DBP), was obtained from Aldrich. It was washed with a 5% aqueous solution of $NaHSO_3$ followed by pure water, dried over $CaCl_2$, and vacuum-distilled prior to use. Solutions were prepared gravimetrically, with the aid of pentane as a cosolvent. The pentane was stripped off under vacuum, at room temperature, until constant weight was achieved. The antioxidant 2,6-di-*tert*-butyl-4-methylphenol was added to each solution (0.3% by weight of polymer). A solution of SIS-120 with weight fraction $w = 0.183$ and a solution of SI-60 with $w = 0.177$ were used extensively for the rheological and flow birefringence measurements. The corresponding volume fractions, ϕ, were estimated to be 0.201 and 0.195, assuming additivity of volumes.

Cloud Point. In order to assess the quality of DBP as a solvent for the PI block, cloud point measurements were performed on solutions of PI homopolymer ($M_w = 6.6 \times 10^4$, $M_w/M_n = 1.02$) at various concentrations. Each solution was prepared with 0.5% antioxidant by weight of PI, and was stirred, under nitrogen, throughout the measurements. Cloud points were assessed by visual inspection, using white light, as the temperature was decreased from 80 °C at 2 °C/min. Each cloud point was determined three times, and the results were averaged. The results indicate a critical concentration of $w \approx 0.10$, and an apparent critical temperature of 77 °C.

Dynamic Light Scattering. DLS measurements were made on a dilute SIS-120 solution, to characterize the micellization behavior in the absence of substantial intermicelle interactions. The solution had $w = 0.005$ and was filtered prior to use. The DLS spectrometer incorporates a commercial goniometer (Malvern), an Ar^+ laser operating at 488 nm, and a Brookhaven BI-9000 correlator. For each solution, intensity correlation functions $g^{(2)}(t)$ were acquired at five different angles from 45 to 120°, and analyzed via the method of cumulants and by the Laplace inversion routine CONTIN.[27] Measurements were performed at 30 ± 0.1 and 60 ± 0.2 °C.

Rheology. Measurements were performed on a Rheometrics Fluids spectrometer (RFS II) using 25 or 12.5 mm diameter parallel plates. Strain amplitudes γ ranged from 0.01 to 1.5, depending on the state of the system; in the ordered state, $\gamma \leq 0.1$. In all cases, it was established that the response was independent of γ. Frequencies, ω, from 0.001 to 100 rad/s were employed, and the temperature was controlled to within ±0.2 deg. A steady flow of nitrogen was employed throughout the measurements, to inhibit possible sample degradation.

Oscillatory Flow Birefringence. The OFB measurements were made on an apparatus described previously.[28,29] The solution is subject to an oscillating shear between parallel plates, and the birefringence is detected with a dual-detector-based optical train, and a digital lock-in data acquisition system, as detailed elsewhere.[30,31] Strain amplitudes were typically much lower than for the rheological measurements. Frequencies from 0.01 to 1000 Hz were employed, and the temperature was controlled to within ±0.02 deg. A steady flow of nitrogen was employed throughout the measurements, to inhibit possible sample degradation.

Small-Angle Neutron Scattering. SANS measurements were performed at the National Institute for Standards and Technology, utilizing a Couette geometry shear cell with a gap width of 0.5 mm. Neutrons with $\lambda = 5.00$ Å, and a sample-to-detector distance of 8.05 m were employed. The contrast factors between the monomers and the solvent are very small, in the absence of deuterium labeling, and so the scattering intensities were rather weak. As the primary goal was to gain

qualitative information about the solution morphology, incoherent and solvent intensities were not subtracted, and the intensity data were not placed on an absolute basis.

Small-Angle X-ray Scattering. Small-angle X-ray scattering (SAXS) experiments were performed on beamlines 2.1 and 8.2 of the Synchrotron Radiation Source (SRS) at the Daresbury Laboratory, Warrington, U.K. Details of the storage ring, radiation, camera geometry, and data collection electronics have been given elsewhere.[32]

On station 2.1, white radiation is monochromated using a bent triangular Ge(111) monochromator to give a high-intensity, fixed wavelength beam with $\lambda = 1.54$ Å. Focusing is achieved in both horizontal and vertical directions by means of the monochromator and a quartz mirror, respectively. A 6 m camera was employed, which gives a q range from 0.005 to 0.13 Å^{-1}. On station 8.2, a cylindrically bent Ge(111) monochromator gives an intense beam with $\lambda = 1.50$ Å. With the SRS operating at 2 GeV and 200 mA, a flux of 4×10^{10} photons/s is generated at the sample, and the beam is highly collimated to a typical cross-section of 0.3×4 mm^2 in the focal plane. A vacuum chamber is placed between the sample and detector to reduce air scattering and absorption; a 3 m sample-to-detector distance was used.

On both stations, detectors that measure intensity in the radial direction (over an opening angle of 70° and an active length of 0.2 m) were used. These are suitable only for isotropic scatterers. The active area increases radially, improving the signal-to-noise ratio at larger angles compared to single wire detectors. The spatial resolution of each detector is 500 μm, and they can handle up to 2.5×10^5 counts/s.

The SAXS samples were prepared by inserting sealed glass capillaries in a Linkam hot-stage mounted to an optical bench. The silver heating block of the hot-stage contains a 4×1 mm^2 tapered slot to allow transmitted and scattered X-rays to pass through unhindered. Cooling was achieved using a Linkam nitrogen flow controller, which also enables control of the heating rate, which was set at 1, 2, or 3 °C/min.

Scattering from an oriented specimen of wet collagen (rat-tail tendon) was used to calibrate the detector. A parallel plate ionization detector placed before the sample cell recorded the incident intensities. The experimental data were corrected for background scattering, sample absorption, and the positional alinearity of the detectors. The data are presented as a function of $q = (4\pi/\lambda) \sin \theta$, where 2θ is the scattering angle.

Results and Discussion

The results are presented in three parts. First, we discuss dilute solution characterization of the micelles formed by the triblock copolymer; second, we address the dynamics of 20% solutions of the triblock and diblock copolymers as a function of temperature; third, we describe characterization of the solution structure via SANS and SAXS. In the discussion that follows, we present a qualitative explanation for the observed phenemona.

Dilute Solution Characterization. At 30 °C, the DLS intensity correlation functions are dominated by a single mode which is close to a single exponential decay. The associated decay rate, Γ, is linear in the square of the wavevector, q, and thus the corresponding process is diffusive. Application of the Stokes−Einstein relation

$$D = \frac{kT}{6\pi\eta_s R_h} \tag{1}$$

and the solvent viscosity (14.3 cP) leads to a hydrodynamic radius, R_h, of 260 Å. This is clearly far in excess of the size of a single coil and corresponds closely to the radii obtained from micelles formed by similar molecular weight triblocks in dilute solutions of a solvent selective for the end blocks.[11,13,17] At 60 °C, however, the equivalent analysis leads to a value for R_h of 100 Å, approximately what one would expect for the single chain. Consequently, one may conclude that the increase in temperature is sufficient to overcome the enthalpic drive toward micellization. This conclusion is confirmed by measurements of the static scattered intensity; the intensity decreases rapidly upon heating, indicating a dilute solution critical micelle temperature of 49 ± 1 °C. This behavior has its origin in the changing solvent quality of DBP toward the isoprene block, rather than in the temperature dependence of the styrene−isoprene interaction parameter, as indicated by the cloud point measurements described in the Experimental Section. For example, when the same triblock is dissolved in dilute solution in putatively neutral good solvents such as toluene and THF, no micellization occurs.[33]

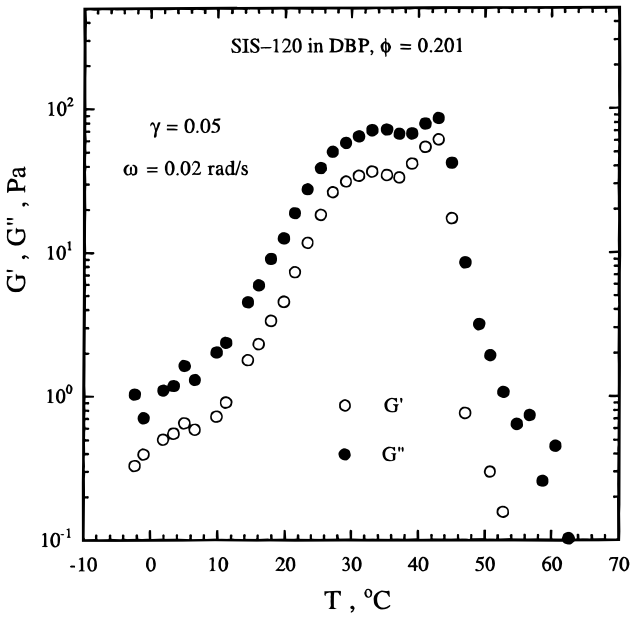

Figure 1. Dynamic shear moduli for the triblock copolymer as a function of temperature.

Dynamic Properties. The most striking feature of the results for this system is illustrated in Figure 1. The low frequency ($\omega = 0.02$ rad/s) and low strain amplitude ($\gamma = 0.05$) dynamic shear moduli, G' and G'', are plotted as a function of increasing temperature for the SIS-120 solution with $\phi = 0.201$. Over the interval from 0 to 40 °C, the moduli increase by about 2 orders of magnitude. This indicates the formation of some new structure and/or the onset of new interactions, in the solution. At 44 °C, there appears a sharp transition, and the moduli drop abruptly. By about 60 °C, the viscosity of the fluid is comparable to that expected for a disordered, entangled polymer solution with this concentration and molecular weight. There are thus (at least) three regimes of behavior to understand: below about 10 °C; from *ca.* 10 to 44 °C; from 44 to *ca.* 60 °C. The low-temperature state will be associated with dispersed micelles, and the high-temperature regime with the gradual dissipation of intermolecular associations, reminiscent of the fluctuation regime for symmetric diblocks in melts and neutral solvents.[34,35] The intermediate regime is, clearly, unusual. As a working hypothesis, we attribute the increase in modulus to the swelling of the micelles, due to the gradual solvation of the PI core by the solvent, which leads to strong physical interactions between closely-packed micelles. We will refer to the transition at 44 °C as the microphase separation

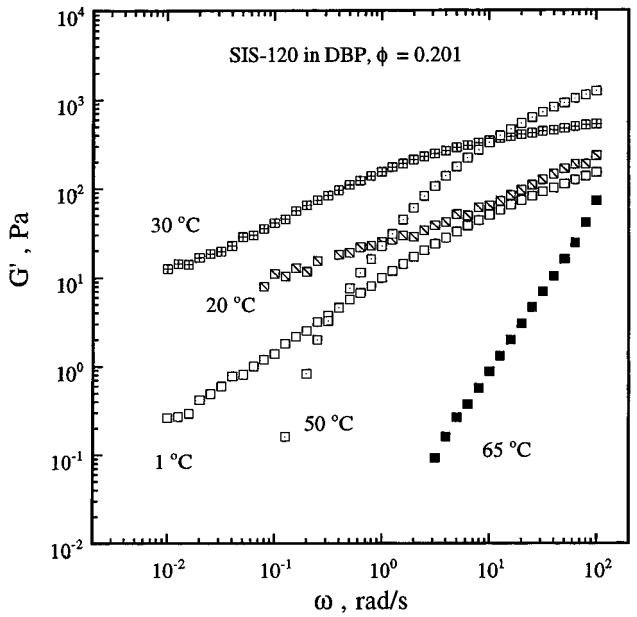

Figure 2. Frequency dependence of the elastic modulus for the triblock copolymer at the indicated temperatures.

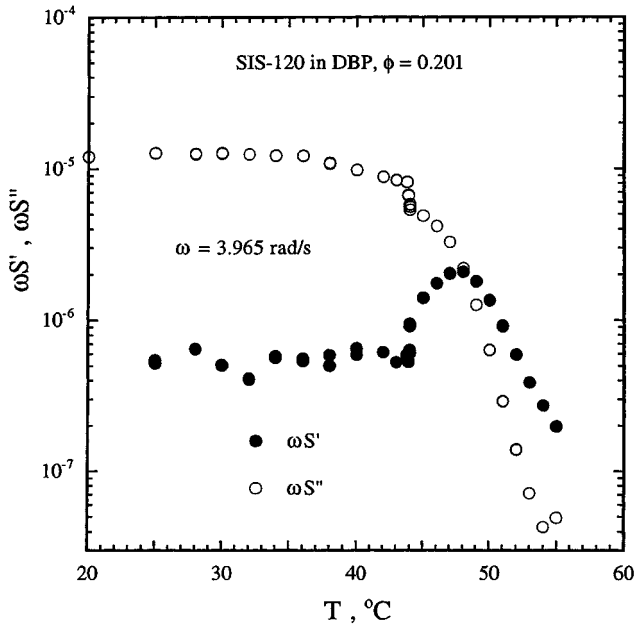

Figure 3. Dynamic flow birefringence properties for the triblock copolymer as a function of temperature.

transition (MST) rather than the order−disorder transition, because there is no clear evidence in the scattering analysis (*vide infra*) of a long range periodic structure or macrolattice.

The frequency dependence of the elastic modulus is shown for the same solution at various temperatures in Figure 2. At 1 °C the low-frequency slope is close to $^3/_4$, clearly not the exponent of 2 associated with the terminal regime for a liquid. By 20 and 30 °C, the modulus has increased substantially, and the low-frequency slope is approximately $^1/_2$. This exponent is similar to that observed in the ordered state of diblock copolymer melts, in the lamellar or cylindrical morphologies.[3] At 50 °C, above the MST, G' superficially resembles a liquid in the terminal regime, but note that the modulus drops by over 2 orders of magnitude upon further heating to 65 °C. Clearly, this temperature dependence above the MST is far too strong for a disordered polymer solution and must reflect a progressive, additional decrease in intermolecular association.

The corresponding OFB properties of the same solution are shown in Figures 3 and 4. The quantities $\omega S'$ and $\omega S''$ would be directly proportional to G'' and G', respectively, for a fluid obeying the stress-optic relation (SOR). Even disordered block copolymer liquids, however, rarely follow a simple SOR.[36,37] In Figure 3, the T dependence of $\omega S'$ and $\omega S''$ shows the same T_{MST} as the rheology, followed by a decrease toward a liquidlike response. However, other features are different: (i) below the transition, the OFB response is almost independent of T; (ii) the elastic component is the larger; and (iii) the transition is distinctly first order in the elastic component. In Figure 4, the optical analog to G' shows the same strong T dependence of the longest relaxation time above the MST.

The magnitude of the birefringence below the MST is over 1 order of magnitude higher than would be expected from a PI homopolymer solution with the same modulus. Furthermore, PI has a positive, and PS a negative, polarizability anisotropy, so that the net copolymer birefringence would be even less than for a PI homopolymer solution. The birefringence exhibited here is positive, and thus it must arise predominantly from form birefringence, due to the different refractive

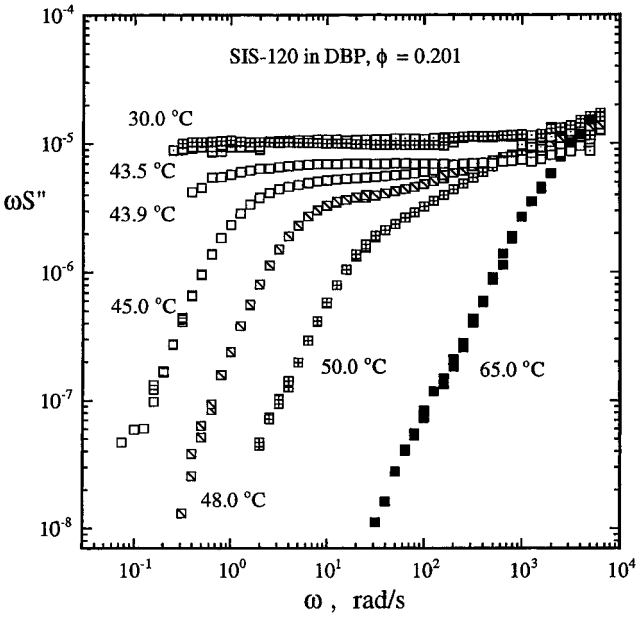

Figure 4. Frequency dependence of the elastic component of the birefringence for the triblock copolymer at the indicated temperatures.

indicies of PI- and PS-rich domains. These results indicate that the morphology is anisotropic; spherical or bicontinuous cubic microstructures would not be expected to give substantial form birefringence, at least under such low strains and strain rates. Furthermore, over the range from 25 to 40 °C there is no evidence of a changing structure with T, in contrast to the moduli. This suggests that the moduli reflect an increasingly strong interaction between domains, or micelles, whereas the birefringence indicates that the fundamental morphology remains roughly constant over this T range.

Figure 5 shows G' for a slightly more dilute solution of SIS-120, $\phi = 0.172$, with measurements taken under both heating and cooling cycles (at *ca.* 0.5−1 °C/min). There is some hysteresis, with an extra shoulder appearing (quite reproducibly) near 30 °C upon heating. However, the hysteresis is not dramatic, indicating that the system is able to remain close to equilibrium

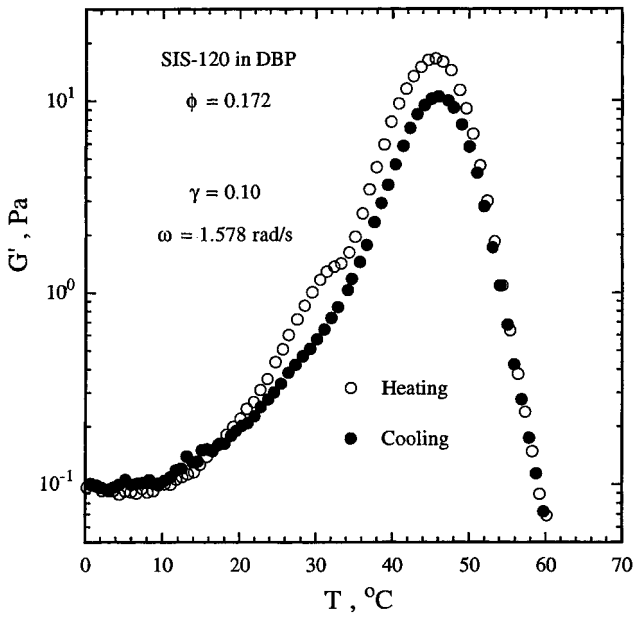

Figure 5. Temperature dependence of the elastic modulus for the triblock copolymer, showing both heating and cooling cycles.

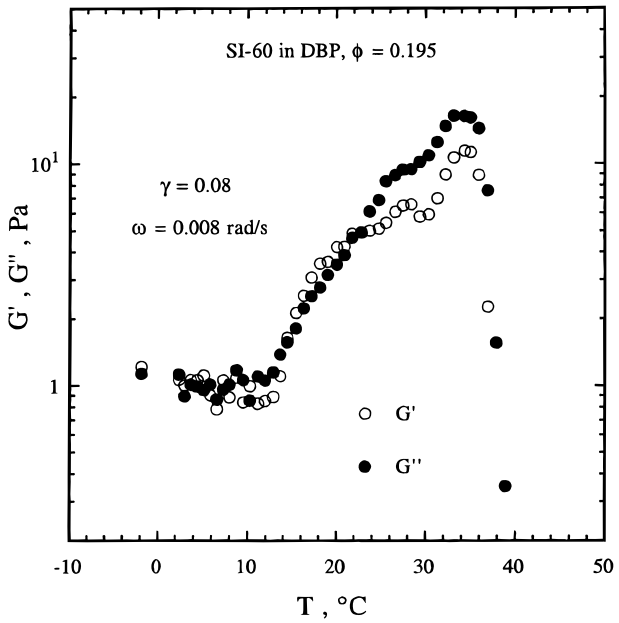

Figure 6. Dynamic shear moduli for the diblock copolymer as a function of temperature.

conditions throughout these measurements. Interestingly, $T_{MST} \approx 45$ °C, even though the polymer concentration has decreased. This suggests strongly that this transition reflects changing solvent quality, rather than simply interactions between PS and PI blocks; in the latter case, decreasing concentration should stabilize the disordered state and decrease T_{MST}. However, the maximum in G' is about a factor of 5 lower than in Figure 1, even though the applied frequency is higher; this reflects a reduction by dilution of the intermolecular interactions responsible for the maxima in the moduli.

Rheological and rheo-optical measurements were performed on an SI-60 solution at a concentration similar to that in Figures 1−4, $\phi = 0.195$. The results for the T dependence of G' and G'' are shown in Figure 6. The gross features are very similar to those for the triblock: the moduli increase with T over the range from 10 to 35 °C, followed by an abrupt transition to a disordered liquid state. Figure 7 shows the T dependence of $\omega S''$ at two frequencies, and the results are also qualitatively similar to those in Figure 3. The birefringence is large and positive below the transition, due to the form birefringence from an anisotropic structure, and then it drops precipitously above $T_{MST} \approx 36$ °C. The magnitude of the birefringence in the ordered state is independent of ω, as in Figure 4. Evidently, the topology of the copolymer (diblock vs triblock) has at most a modest influence on the resulting viscoelastic properties. This is important, because it eliminates "temporary network" or "gel-like" structures formed by the triblock as possible explanations for the maxima in the moduli. Of course, as DBP is a good solvent for PS, one would not have expected association of the PS blocks to be significant in these solutions.

Structural Characterization. Representative SANS data for the SI-60 solution are shown in Figure 8, as $I(q)$ versus q. The data were taken under shear, and the results azimuthally averaged. There is a distinct peak in $I(q)$, with a maximum at a q^* that decreases with increasing T. $I(q^*)$ grows substantially with decreasing T, indicating an increasing segregation of styrene-rich and isoprene-rich microdomains. This

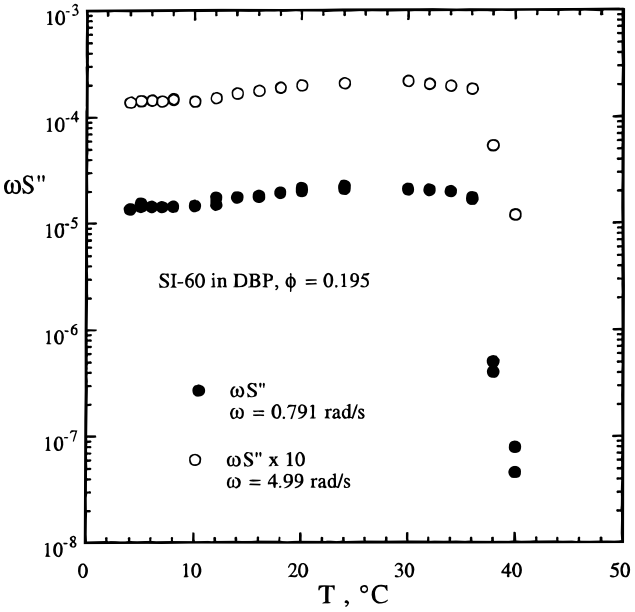

Figure 7. Dynamic flow birefringence properties for the diblock copolymer as a function of temperature.

should be compared with the low-frequency moduli, which increase with T over the same range. The three higher T data sets in Figure 8 were obtained at a rotation rate of 0.1 rps, whereas the lower two had a rotation rate of 0.5 rps. The effect of rotation rate on the azimuthally-averaged scattered intensity is rather weak, and so this difference is not significant. The azimuthal angle dependence of the peak intensity, $I(q^*)$, is shown for the same solution in Figure 9, at three temperatures. At 45 °C, above the rheological MST, there is at most a small asymmetry, but at lower T there is clearly an oriented structure in solution. The symmetry is consistent with cylinders, elongated micelles, or even lamellae, oriented primarily along the flow direction. No evidence for a bcc lattice, or any periodicity in other directions, was detected. The anisotropy at a given T was greater at 0.1 rps than at 0.5 rps. Qualitatively similar results were obtained for an SIS-120 solution, except that under otherwise equivalent

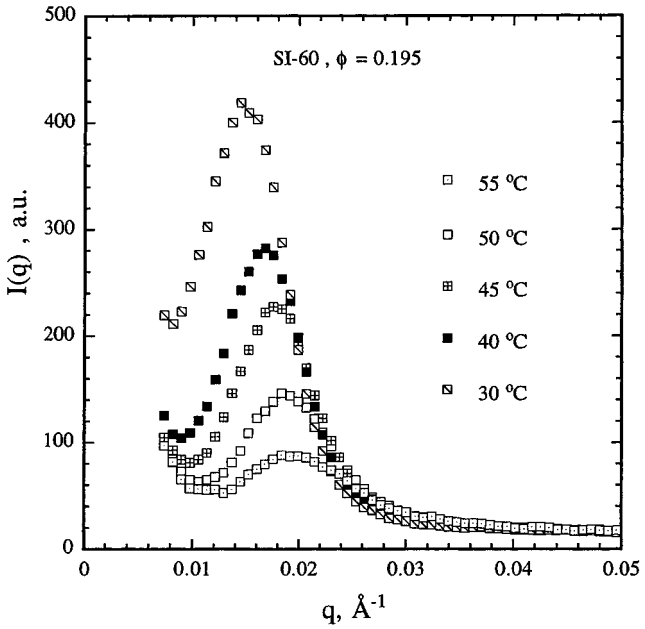

Figure 8. Azimuthally-averaged SANS intensity as a function of wavevector for the diblock copolymer under shear.

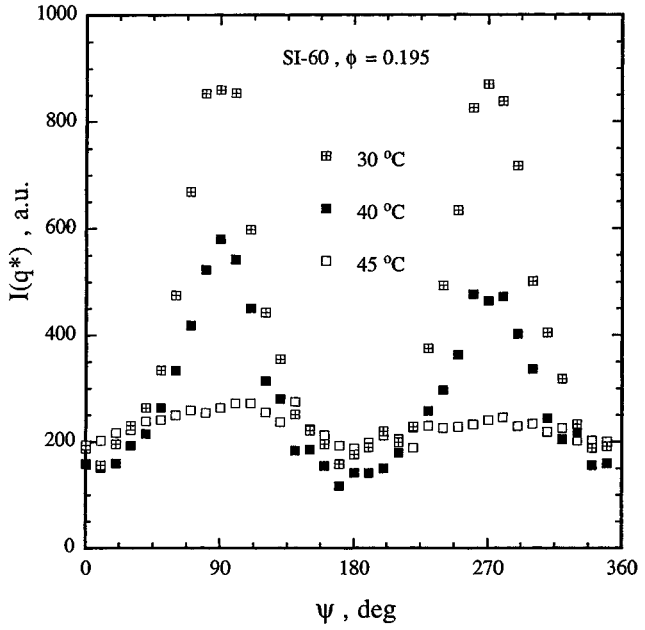

Figure 9. Angular dependence (relative to the shear direction) of the SANS intensity at q^* for the diblock copolymer.

conditions the diblock solution achieved a higher degree of orientation.

SAXS data for the SIS-120 solution ($\phi = 0.201$) taken during a heating ramp at 3 °C/min from −35 to +90 °C are shown in Figure 10. At low temperatures, oscillations can be observed in the high-q portion of the data that arise from the form factor of isolated micelles (we return to a discussion of a model for the micelle structure shortly). A single peak arising from the liquid structure factor is evident at $q^* = 0.010-0.011$ Å^{-1} for $T < 0$ °C, the peak position moving slightly to higher q with increasing temperature. The location of the first maximum in the form factor scattering is also weakly dependent on temperature in this range. The values of q^* from SAXS are slightly smaller than those from SANS, for reasons that are not immediately apparent. However, given the qualitative nature of the SANS

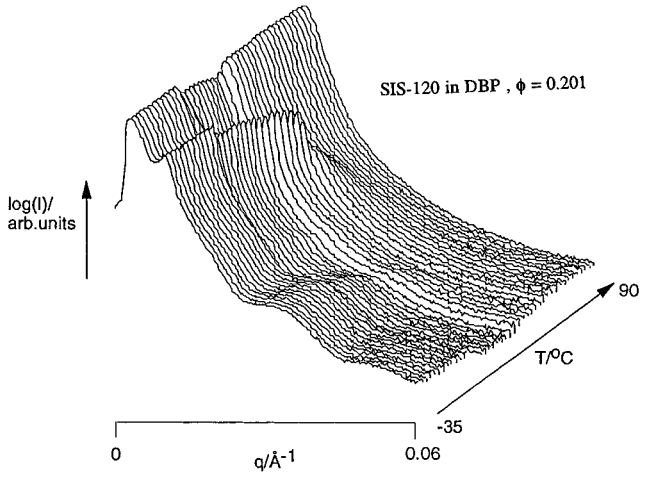

Figure 10. SAXS intensity for the triblock copolymer as a function of wavevector, over the indicated temperature range.

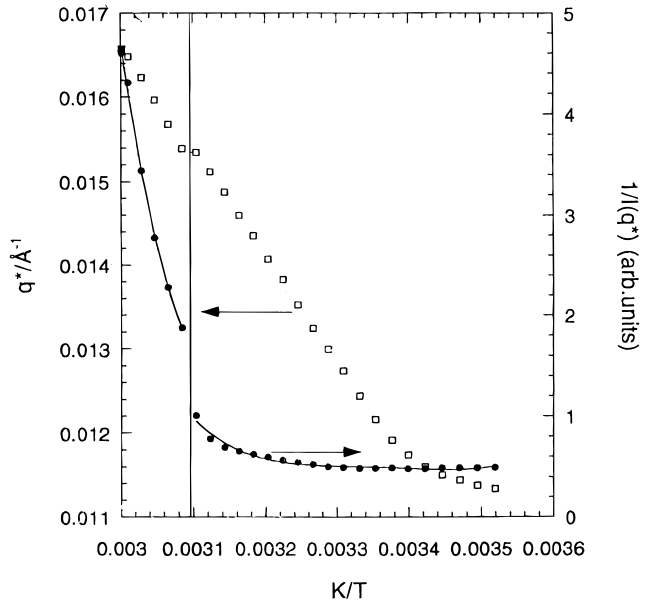

Figure 11. SAXS peak position, q^*, and inverse peak intensity as a function of inverse temperature, for the triblock copolymer.

analysis, the SAXS values are considered more significant.

The T dependence of the location of the structure factor peak, q^*, and of the inverse intensity at q^* over the temperature range 10−60 °C, are shown for this sample in Figure 11. These data are plotted against T^{-1} to facilitate comparison with results from block copolymer melts. In that case, the I^{-1} would be expected to scale linearly with T^{-1} in the mean-field approximation. This follows from the mean-field equation for the inverse intensity

$$\frac{N}{I(q)} \sim F(q) - 2\chi N \qquad (2)$$

where $F(q)$ is a function of radius of gyration and composition of the block copolymer.[38] This function has a minimum, and hence $I(q)^{-1}$ has a maximum, at $q = q^*$, which is independent of χ and thus T. Empirically, χ is found to be inversely proportional to temperature: $\chi = A + B/T$, where A and B are constants. Thus $I(q^*)^{-1}$ should change linearly with T^{-1}, and the same scaling is also predicted for q^*. A scaling similar to eq

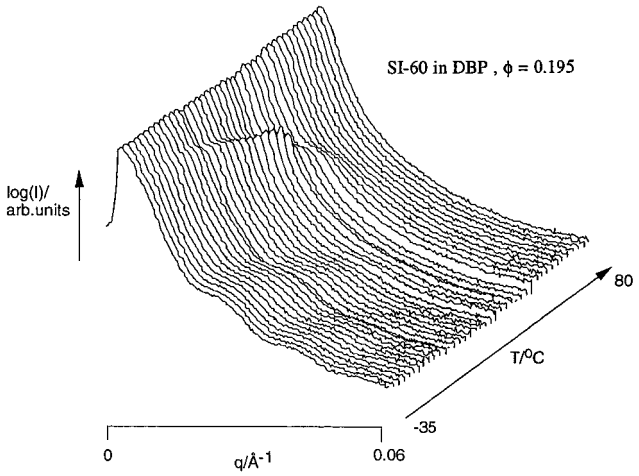

Figure 12. SAXS intensity for the diblock copolymer as a function of wavevector, over the indicated temperature range.

2 was obtained by Fredrickson and Leibler and by Olvera de la Cruz from a mean-field analysis of microphase separation in semidilute solutions of block copolymers in nonselective good solvents, with the block copolymer composition $f \sim 0.5$.[39,40] Although DBP is not a neutral solvent, and the copolymer composition is not close to $f = 0.5$, it is interesting to note that an almost linear scaling of I^{-1} with T^{-1} is obtained.

The data on heating for the SIS-120 solution show a clear break in I^{-1} and $\partial q^*/\partial T$ at one temperature, which, following work on block copolymer melts, we identify as the MST. The SAXS T_{MST} is determined to be 50 ± 1 °C. Although there is a significant hysteresis associated with this transition (during the cooling ramp at 1 °C/min, discontinuities in $\partial q^*/\partial T$ and $1/I(q^*)$ were not observed), T_{MST} is reproduced on subsequent heating runs (performed 2 h later and 5 months later), as were the discontinuities. The SAXS value for T_{MST} is in close agreement with the value from rheology. The nonlinearity in the high-temperature data is indicative of the presence of composition fluctuations,[34,41] as also inferred from the rheological and OFB data. There is also a discontinuous change in the intensity of the scattering in the Guinier regime at the edge of the beamstop in these data at the MST. The amplitude of the structure factor oscillations decays smoothly as the temperature is increased, a feature that we associate with an increasing diffuseness of the micelle structure. At temperatures above 60 °C the structure factor peak and the form factor oscillations disappear, which we associate with the final dissociation of the block copolymer micelles as the chains go into a homogeneous solution.

SAXS profiles for the SI-60 solution ($\phi = 0.195$) in the temperature range −35 to +80 °C are shown in Figure 12. In contrast to the data for the triblock solution, at low temperatures there is no structure factor peak at low q. However, there are oscillations as a function of q, indicating a micellar structure. The absence of a structure factor peak suggests that there is no intermicellar ordering, and the solution consists of an effective gas of micelles. At temperatures above 10 °C a structure factor peak begins to develop from a shoulder into a separate peak at low q. The dependence of the position of the maximum of this peak, q^*, and $1/I(q^*)$ are plotted against T^{-1} in Figure 13. As with the SIS-120 solution, breaks in both q^* and $I(q^*)$ occur at the same temperature, $T_{MST} = 36 \pm 1$ °C. The discontinuity appears less pronounced than for the triblock solution, simply because a data point was taken

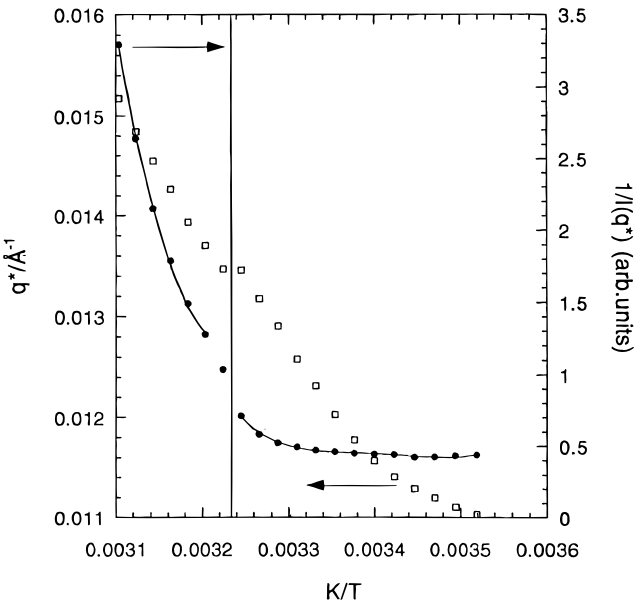

Figure 13. SAXS peak position, q^*, and inverse peak intensity as a function of inverse temperature, for the diblock copolymer.

very close to the MST. The transition temperature, and the discontinuities, are reproducible on successive heating ramps although, as for the triblock solution, there is some hysteresis associated with the heating/cooling cycle. The SAXS value for T_{MST} is identical to the value from rheology and OFB. As with the triblock, the form factor oscillations decrease in magnitude with increasing temperature, due to the broadening of the interfacial composition profile. The structure factor peak for this sample disappears between 43 and 49 °C; over this temperature range the block copolymer chains dissociate into a homogeneous solution.

The model that has been used for analyzing the SAXS data is based on the assumption of a micelle with a dense PI core, surrounded by a corona of solvated PS chains. It further emerges from the fitting that the micellar cores have elliptical shapes, which is in agreement with the observations of shear alignment in SANS and form birefringence in OFB. A detailed description of the model for spherical cores has been given,[42] whereas the details of the extension to elliptical and cylindrical micelles will be presented elsewhere.[43] The PI core is assumed to be homogeneous, and the PS chains are assumed to follow Gaussian statistics. Technically, the calculation allows the PS chains to penetrate the PI core, an unphysical feature that leads to a change in the distribution of the PS chains. However, Monte Carlo simulations have shown that these changes can be captured accurately by moving the starting points of the PS chains a distance d away from the surface. This distance $d = \beta R_g$, where β is a constant of order unity and R_g is the radius of gyration of the chains.

The form factor of the micelle contains four different terms: the self-correlation of the core, the self-correlation of the chains, the cross-term between the core and chains, and the cross-term between different chains. It can be written[42]

$$F_{mic}(q) = N_{agg}{}^2\rho_s{}^2F_s(q,R,\epsilon) + N_{agg}\rho_c{}^2F_c(q,L,b) + N_{agg}(N_{agg} - 1)\rho_c{}^2S_{cc}(q) + 2N_{agg}{}^2\rho_s\rho_cS_{sc}(q) \quad (3)$$

where N_{agg} is the aggregation number of the micelle and ρ_s and ρ_c are the total excess scattering length of the

(PI) blocks in the core and of the dissolved (PS) chains, respectively. The elliptical core has the semiaxes (R, R, ϵR) and the chains have contour length L and Kuhn length b. The normalized self-correlation term [$F_c(q=0,R,\epsilon)=1$] for the elliptical core is given by[44]

$$F_c(q,R,\epsilon) = \int_0^{\pi/2} \Phi^2[q,r(R,\epsilon,\alpha)] \sin\alpha \, d\alpha \qquad (4)$$

where $r(R,\epsilon,\alpha) = R(\sin^2\alpha + \epsilon^2\cos^2\alpha)^{1/2}$ and

$$\Phi(q,r) = \frac{3[\sin(qr) - qr\cos(qr)]}{(qr)^3} \qquad (5)$$

The self-correlation term of the Gaussian chains is given by the Debye function:

$$F_c(q,L,b) = \frac{2}{x^2}[\exp(-x) - 1 + x] \qquad (6)$$

where $x = q^2R_g^2$ and $R_g^2 = Lb/6$. The interference cross-term between the core and Gaussian chains starting at d away from the surface of the core is

$$S_{sc}(q) = \psi(q,L,b)\int_0^{\pi/2} \Phi(q,r)\frac{\sin(q[d+r])}{q[d+r]} \sin\alpha \, d\alpha \qquad (7)$$

The function $\psi(q,L,b) = x^{-1}[1 - \exp(-x)]$ is the form factor amplitude of the chain.[45] Finally, the interference term between the chains is

$$S_{cc}(q) = \psi^2(q,L,b)\int_0^{\pi/2} \left[\frac{\sin(q[d+r])}{q[d+r]}\right]^2 \sin\alpha \, d\alpha \qquad (8)$$

The SAXS data of the SIS-120 ($\phi = 0.201$) and the SI-60 ($\phi = 0.195$) solutions at −35 °C have been analyzed by least-squares fitting to the model. As the specific densities of the polymer and the solvent are not known as a function of temperature, the ratio between the excess scattering length densities was kept as a fitting parameter. The Kuhn length was fixed at 25 Å, and the contour was estimated as $L = N_{PS}l_0 = 241$ Å from the degree of polymerization, N_{PS}, and the contour length per PS monomer, $l_0 = 2.51$ Å. The aggregation number, N_{agg}, and the eccentricity of the micelles, ϵ, were fitting parameters. From these two parameters the radius R of the micelle core was calculated from

$$N_{agg}N_{PI}V_{PI} = \frac{4\pi}{3}\epsilon R^3 \qquad (9)$$

where $V_{PI} = 125.5$ Å^3 is the volume of one monomer. The last fitting parameter is the constant β, giving a total of five fitting parameters: (ρ_s/ρ_c), N_{agg}, ϵ, β, and an overall scale factor.

Plots of the fits to the experimental data are shown, in double logarithmic format, in Figures 14 and 15, for SIS-120 and S-60, respectively. The model reproduces the experimental data quite well. For SIS-120 there is a peak at about $q = 0.011$ Å^{-1}, which is due to the solution structure factor. As this is not included in the model, this peak is not reproduced by the fit. There are additional small deviations between the fit and the data in the q region where the oscillations occur. This is attributable to polydispersity in the micellar size, which is also not taken into account.[42] The best least-squares fit for SIS-120 gave $R = 150$ Å, $\epsilon = 3.8$, $N_{agg} = 295$, $\beta = 0.05$, and $\rho_s/\rho_c = 2$, and for SI-60 $R = 197$ Å, $\epsilon = 2.7$, $N_{agg} = 940$, $\beta = 0.14$, and $\rho_s/\rho_c = 1.8$. The micelles are thus prolate ellipsoids. The various parameters in the fit interact to a considerable degree, and thus other solution sets are conceivable. However, the values of ϵ needed to be greater than 2.5 for SIS-120 and 2 for SI-60, in order to achieve satisfactory agreement. Thus, the anisotropy of the micelles is confirmed, in agreement with the SANS and OFB results. Exact values for the length of the major axes cannot be established, due to the lack of scattering data at lower q, and the (presumed) polydispersity in micelle length. The scattering density ratios are reassuringly similar for the two samples, but the values of the ratio are not particularly significant, in that the contrast among PI, PS, and DBP is small, and thus very sensitive to the exact values of the respective specific volumes. Finally, it should be noted that the micelle dimensions are insensitive to the assumption of no solvent in the core.

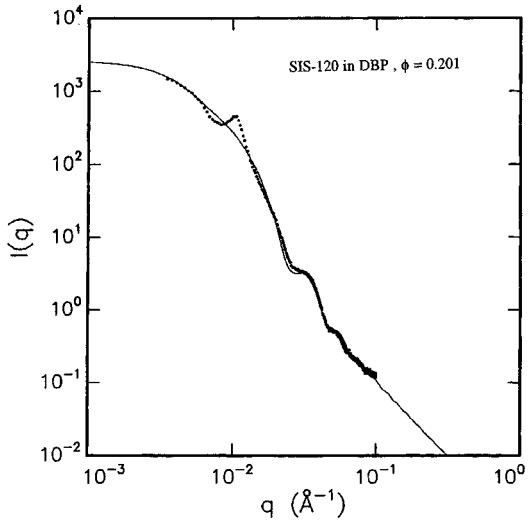

Figure 14. SAXS intensity as a function of wavevector, and fit of the ellipsoidal micelle model, for the triblock copolymer at −35 °C.

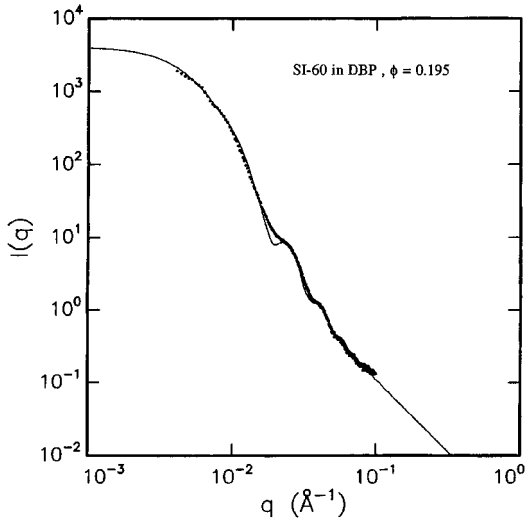

Figure 15. SAXS intensity as a function of wavevector, and fit of the ellipsoidal micelle model, for the diblock copolymer at −35 °C.

Discussion. The various phenomena described above may be reconciled by the following picture. At low temperatures, the copolymers assemble into micelles with PI-rich cores. These micelles are anisotropic, as evidenced both by SANS under shear and OFB. The detailed SAXS analysis supports a model of prolate ellipsoids, with an average aspect ratio of about 3.

However, the micelles are presumably polydisperse, both in size and in shape. Although the fits to the scattering profiles are not unique, and other structures are conceivable, the ellipsoidal model gave much better fits than either spherical or cylindrical (worm-like) micelles. The minor axis of the core for SIS-120, 150 Å, combined with an estimated corona thickness of 60 Å (based on $2R_g$ for PS with $M = 10^4$), is reasonably consistent with the hydrodynamic radius of 260 Å obtained by DLS in dilute solution. Whether the micelles are similarly anisotropic in dilute solution is not known, but there is no *a priori* reason to expect a change in micelle shape with increasing concentration above the cmc. The fact that the micelles are elongated reflects the molecular asymmetry; in a spherical micelle, the PI chains would be more confined, and the PS chains "grafted" to the core surface would be more dilute. Increasing the PS molecular weight for a fixed PI size would increase the steric interactions within the corona, eventually driving a transition to a spherical morphology. The SAXS structure factor peak at low temperatures occurs near 0.011 $Å^{-1}$, which we interpret, at least qualitatively, as an estimate of the minimum intermicellar separation of $2\pi/q^* \approx 570$ Å, *i.e.*, greater than two micellar radii (*ca.* 520 Å for SI-60 and 420 Å for SIS-120). This is consistent with the conclusion from rheology that intermicellar interactions are weak in this regime.

As temperature increases, the viscoelastic properties indicate the onset of strong intermicellar interactions at about 10 °C. This can be attributed to swelling of the PI cores by the solvent. Although the solution is well below T_c for PI in DBP, the relevant part of the PI/DBP phase diagram is the high polymer concentration regime, where the coexistence curve lies at much lower temperatures than T_c (for a UCST system). Dilution of the core would lead to a smearing of the core/corona interface, and a reduction in scattering contrast. Both of these features are apparent in the SAXS results, where the form factor oscillations and the peak intensity diminish with increasing temperature. The SANS $I(q^*)$ also shows the same trend with temperature (note that PS and DBP are almost contrast-matched, whereas PI provides some contrast to either PS or DBP).

The solvation of the core could result in both a lateral swelling and an increase in the average length of the micelles. The results favor the latter, for the following reason. Experimentally, the peak in the structure factor moves to larger q, implying that the centers of the micelles are approaching one another more closely. For example, by the MST, the minimum intermicellar spacing is *ca.* 465 Å for SIS-120 and 400 Å for SI-60, which would correspond to significant overlap of the coronas. For the centers of the micelles to approach one another more closely on average (in the absence of attractive micelle-micelle interactions), there must be either an increase in the number of micelles of fixed dimension, which is not possible because the polymer concentration is fixed, or an elongation of the average micelle, which forces micelles closer together in the two directions orthogonal to the major axis. In contrast, if lateral swelling were dominant, one would expect q^* to remain roughly constant, even though the rheological consequences might be similar. Elongation of anisotropic micelles by solvent swelling of the core is intuitively reasonable, especially for the triblock. Lateral swelling would, ultimately, incur an entropic stretching penalty for the core chains, whereas expansion along the major axis permits the core chains to adopt more preferred conformations.

The strong increase in the moduli due to the closer packing of the micelles could be due either to elongation of the average micelle or to the coronal overlap. By analogy to entangled polymer solutions, the former would correspond to increasing molecular weight at fixed concentration, and the latter to increasing concentration at fixed molecular weight. In concentrated solutions of flexible polymers, the viscosity increases roughly as $(cM)^x$, with x between 3 and 4. Thus, the 2 order of magnitude increase in the moduli observed here would be attributed to a change in average micelle length by a factor of 3. Or, as is more likely the case, both factors are operative, and thus the length change need not be so great. However, it is worth noting that the PS chains are well below the entanglement threshold, and thus entanglement of the corona chains is not a factor.

The MST corresponds to the dissolution of the micelles as the increasing solubility of the isoprene block yields to the entropy of mixing. As noted above, the transition is reminiscent of the ODT in block copolymer melts. It is first order in nature, being accompanied by small but distinct discontinuities in $I(q^*)$ and $\partial q^*/\partial T$ at T_{MST}, and, at least for the triblock, in the birefringence. The inverse intensity above the transition is not exactly linear in inverse temperature and follows a functional form observed in copolymer melts, attributable to composition fluctuations. These fluctuations are apparent in both the scattering and the dynamic experiments and persist for about 10−20 deg above T_{MST}. However, it is interesting to note that this is a rather small window, relative to that reported for solutions of symmetric styrene−isoprene diblocks in a neutral good solvent.[35,46]

Acknowledgment. This work was supported in part by NATO, through award CRG/940078 to I.W.H. and T.P.L., by the National Science Foundation (Grant Number DMR-9018807 to T.P.L.), and by the Center for Interfacial Engineering, an NSF-sponsored Engineering Research Center at the University of Minnesota. Funding was provided for J.P.A.F. under EPSRC contract GR/K05982 to A.J.R. and I.W.H. Beam time at Daresbury was provided by the EPSRC through the Materials SESS. J. Barker and C. J. Glinka provided assistance with the SANS measurements, and S. Slawson and B. U. Komanschek contributed to the SAXS experiments. P. Weimann graciously provided the PI homopolymer.

References and Notes

(1) Tuzar, Z.; Kratochvil, P. In *Surface and Colloid Science*; Matijevic, E. Ed.; Plenum Press: New York, 1993; Vol. 15.
(2) Bates, F. S.; Fredrickson, G. H. *Annu. Rev. Phys. Chem.* **1990**, *41*, 525.
(3) Fredrickson, G. H.; Bates, F. S. *Annu. Rev. Mater. Sci.* **1996**, *26*, 503.
(4) Lodge, T. P.; Pan, C.; Jin, X.; Liu, Z.; Zhao, J.; Maurer, W. W.; Bates, F. S. *J. Polym. Sci., Polym. Phys. Ed.* **1995**, *33*, 2289.
(5) Mayes, A. M.; Barker, J. G.; Russell, T. P. *J. Chem. Phys.* **1994**, *101*, 5213.
(6) Shibayama, M.; Hashimoto, T.; Hasegawa, H.; Kawai, H. *Macromolecules* **1983**, *16*, 1427.
(7) Hashimoto, T.; Shibayama, M.; Kawai, H. *Macromolecules* **1983**, *16*, 1093.
(8) Raspaud, E.; Lairez, D.; Adam, M.; Carton, J.-P. *Macromolecules* **1994**, *27*, 2956.
(9) Balsara, N. P.; Tirrell, M.; Lodge, T. P. *Macromolecules* **1991**, *24*, 1975.
(10) Tuzar, Z.; Kratochvil, P. *Makromol. Chem.* **1972**, *160*, 301.

(11) Plestil, J.; Baldrian, J. *Makromol. Chem.* **1973**, *174*, 183.
(12) Tuzar, Z.; Plestil, J.; Konak, C.; Hlavata, D.; Sikora, A. *Makromol. Chem.* **1983**, *184*, 2111.
(13) Prochazka, O.; Tuzar, Z.; Kratochvil, P. *Polymer* **1991**, *32*, 3038.
(14) Plestil, J.; Hlavata, D.; Hrouz, J.; Tuzar, Z. *Polymer* **1990**, *31*, 2112.
(15) Xu, R.; Winnik, M. A.; Hallett, F. R.; Riess, G.; Croucher, M. D. *Macromolecules* **1991**, *24*, 87.
(16) Qin, A.; Tian, M.; Ramireddy, C.; Webber, S. E.; Munk, P.; Tuzar, Z. *Macromolecules* **1994**, *27*, 120.
(17) Villacampa, M.; Quintana, J. R.; Salazar, R.; Katime, I. *Macromolecules* **1995**, *28*, 1025.
(18) Nagarajan, R.; Ganesh, K. *J. Chem. Phys.* **1989**, *90*, 5843.
(19) Watanabe, H.; Kotaka, T. *Polym. Eng. Rev.* **1984**, *4*, 73.
(20) Mortensen, K.; Pedersen, J. S. *Macromolecules* **1993**, *26*, 805.
(21) Mortensen, K. *Europhys. Lett.* **1992**, *19*, 599.
(22) Linse, P. *J. Phys. Chem.* **1993**, *97*, 13896.
(23) Schillen, K.; Brown, W.; Johnsen, R. M. *Macromolecules* **1994**, *27*, 4825.
(24) Bates, F. S.; Schulz, M. F.; Khandpur, A. K.; Förster, S.; Rosedale, J. H.; Almdal, K.; Mortensen, K. *Faraday Discuss Chem. Soc.* **1994**, *98*, 7.
(25) Sakurai, S.; Momii, T.; Taie, K.; Shibayama, M.; Nomura, S. *Macromolecules* **1993**, *26*, 485.
(26) Sakurai, S.; Hashimoto, T.; Fetters, L. J. *Macromolecules* **1996**, *29*, 740.
(27) Provencher, S. W. *Comput. Phys. Commun.* **1982**, *27*, 229.
(28) Sahouani, H.; Lodge, T. P. *Macromolecules* **1992**, *25*, 5632.
(29) Amelar, S.; Eastman, C. E.; Morris, R. L.; Smeltzly, M. A.; Lodge, T. P.; von Meerwall, E. D. *Macromolecules* **1991**, *24*, 3505.
(30) Morris, R. L.; Lodge, T. P. *Anal. Chim. Acta* **1986**, *189*, 183.
(31) Amelar, S.; Krahn, J. R.; Hermann, K. C.; Morris, R. L.; Lodge, T. P. *Spectrochim. Acta Rev.* **1991**, *14*, 379.
(32) Bras, W.; Derbyshire, G. E.; Ryan, A. J.; Mant, G. R.; Felton, R. A.; Lewis, R. A.; Hall, C. J.; Greaves, G. N. *Nucl. Instrum. Methods Phys. Res.* **1993**, *A326*, 587.
(33) Liu, Z.; Kobayashi, K.; Lodge, T. P. Unpublished results.
(34) Bates, F. S.; Rosedale, J. H.; Fredrickson, G. H. *J. Chem. Phys.* **1990**, *92*, 6255.
(35) Jin, X.; Lodge, T. P. *Polym. Prepr. (Am. Chem. Soc., Div. Polym. Chem.)* **1995**, *36* (1), 168.
(36) Lodge, T. P.; Amelar, S. *Rheol. Acta* **1992**, *31*, 32.
(37) Man, V. F.; Schrag, J. L.; Lodge, T. P. *Macromolecules* **1991**, *24*, 3666.
(38) Leibler, L. *Macromolecules* **1980**, *13*, 1602.
(39) Fredrickson, G. H.; Leibler, L. *Macromolecules* **1989**, *22*, 1238.
(40) Olvera de la Cruz, M. *J. Chem. Phys.* **1989**, *90*, 1995.
(41) Fredrickson, G. H.; Helfand, E. *J. Chem. Phys.* **1987**, *87*, 697.
(42) Pedersen, J. S.; Gerstenberg, M. C. *Macromolecules* **1996**, *29*, 1363.
(43) Gerstenberg, M. C.; Pedersen, J. S. Manuscript in preparation.
(44) Guinier, A.; Fournet, G. *Small Angle Scattering of X-rays*; Wiley: New York, 1955.
(45) Hammouda, B. *J. Polym. Sci., Polym. Phys. Ed.* **1992**, *30*, 1387.
(46) Lodge, T. P.; Xu, X.; Jin, X.; Dalvi, M. C. *Makromol. Chem., Macromol. Symp.* **1994**, *79*, 87.

MA9604404